The 3D-structure of a natural inhibitor of cell adhesion molecule expression

Ulrich Hommel[a,*], Hans-Peter Weber[b,*], Lukas Oberer[a], Hans Ulrich Naegeli[a], Berndt Oberhauser[c], Carolyn A. Foster[c]

[a]*Sandoz Pharma AG, Preclinical Research, CH-4002 Basle, Switzerland*
[b]*Nova Research Services, CH-4143 Dornach 1, Switzerland*
[c]*Sandoz Research Institute, A-1235 Vienna, Austria*

Received 18 October 1995; revised version received 28 November 1995

Abstract The three-dimensional structure of cyclopeptolide HUN-7293, a naturally-occurring inhibitor of cell adhesion molecule expression, has been determined from nuclear magnetic resonance data recorded in solution and from X-ray diffraction analysis of single crystals. The backbone conformation of HUN-7293 is characterized by two *cis*-peptide bonds in both the solution and crystalline state. Differences between the solution and crystal structure are visible for the orientation of some side chains and the strength of two transannular hydrogen bonds. Such structural information helps to provide insight into the molecular architecture of HUN-7293 on the atomic level and opens the way for structure-based modifications of this novel inhibitor of cell adhesion molecule expression.

Key words: Conformation; Adhesion molecules; ICAM-1; VCAM-1; Nuclear magnetic resonance; X-Ray crystallography

1. Introduction

Cell adhesion molecules such as ICAM-1, VCAM-1, and E-selectin play a critical role in the immune response by regulating leucocyte migration and cell-to-cell interaction [1,2]. Modulation of these interactions by blocking or inhibiting adhesion molecule expression would have a therapeutic potential in a variety of inflammatory diseases. While searching for low molecular weight inhibitors of inducible adhesion molecule expression, we identified the naturally-occurring compound HUN-7293 in a HaCaT keratinocyte-based ICAM-1 ELISA [3]. HUN-7293 also potently suppresses cytokine-induced expression of VCAM-1 on human endothelial cells [4]. The compound is a fungal product [5] and belongs to a novel class of seven-membered cyclic peptolides that contains several uncommon constituents (i.e. D-2-hydroxy-4-cyanobutyric acid, *N*1′-methoxy-*N*-methyltryptophan and the novel 'C9-amino acid' D-propylleucine). A schematic representation of the chemical constitution of HUN-7293 is shown in Fig. 1.

Macrocyclic natural products have attracted wide interest for the development of drugs in many disease areas [6–8]. However, major problems are associated with these compounds either when they are peptidic in nature resulting in reduced plasma stability, or stereochemically complex, rendering a total synthesis very difficult. As a consequence, much effort has been expended to design and synthesize small molecular mimetics with equal potency and increased chemical stability. Information on the three-dimensional conformation of a compound provides the rational basis for applying molecular modelling techniques [9–10]. To gain insight into the structural basis for the biological activity of HUN-7293, we determined its three-dimensional structure both in solution and in single crystals by NMR spectroscopy and X-ray diffraction techniques, respectively. This approach revealed that HUN-7293 adopts a single well-defined conformation in solution, which is very similar to that found in single crystals.

2. Materials and methods

2.1. NMR spectroscopy and solution structure determination

All spectra were recorded on either a Bruker DMX500 or AM500 spectrometer operating at 500 MHz. Peptolide solutions were typically 2–5 mM in 80% $CDCl_3$/20% (D_6)DMSO or 70% MeOH/30% H_2O mixtures. A constant temperature of 4°C or 15°C was maintained during experiments for ROESY [11] spectra (mixing time = 150 ms), from which structural information was extracted. Isolation and purification of HUN-7293, together with the spectroscopic characterization, will be published elsewhere.

Assigned peaks in ROESY spectra were integrated using XEASY [12] and converted into interatomic distances using CALIBA [13]. Dihedral restraints and stereospecific assignments were incorporated during the process of structure refinement after inspection of structures with low energy and low residual violations of the distance restraints using GLOMSA [13]. The procedure for calculating structures followed standard simulated annealing protocols as described in the X-PLOR Manual 3.0 [14]. A starting structure for X-PLOR runs was generated from DIANA [13] based on a modified library containing the uncommon amino acids *N*-methylalanine (MALA), D-2-hydroxy-4-cyanobutyric acid (DGCN), *N*-methylleucine (MLEU), *N*1′-methoxy-*N*-methyltryptophan (MTO). For simplicity reasons, the 'C9-amino' acid D-propylleucine was substituted by leucine since no structurally-relevant constraints have been found for any protons beyond the D-methyl groups. The absolute configuration of the Ca-atoms of LEU_5 and DGCN_2 was of the L- and D-type, respectively, as determined by chiral phase gas chromatography (data not shown). For all other residues the L-type was assumed, and later confirmed, by the X-ray diffraction analysis described below.

2.2. X-Ray crystallography

Crystals were obtained from a saturated solution in 80% DMSO/20% glycerol after seeding and cooling from 60°C to room temperature at a rate of 1°C/h. The crystals were collected by filtration, washed with water and dried at room temperature in vacuo (10^{-3} mbar). The space group was $P2_12_12_1$, cell dimensions a = 10.36 Å, b = 23.69 Å, c = 25.31 Å, V = 6212 Å^3, Z = 4 (one molecule per asymmetric unit), d_{calc} = 1.128

*Corresponding authors. Fax: (41) (61) 324-5930.

Abbreviations: DGCN, D-2-hydroxy-4-cyanobutyric acid; ICAM-1, intercellular adhesion molecule-1; MALA, *N*-methylalanine; MLEU, *N*-methylleucine; MTO, *N*1′-methoxy-*N*-methyltryptophan; NMR, nuclear magnetic resonance; NOE, nuclear Overhauser effect; PrLEU, propylleucine; ROESY, rotating frame cross-relaxation spectroscopy; VCAM-1, vascular cell adhesion molecule-1.

SSDI 0014-5793(95)01453-5

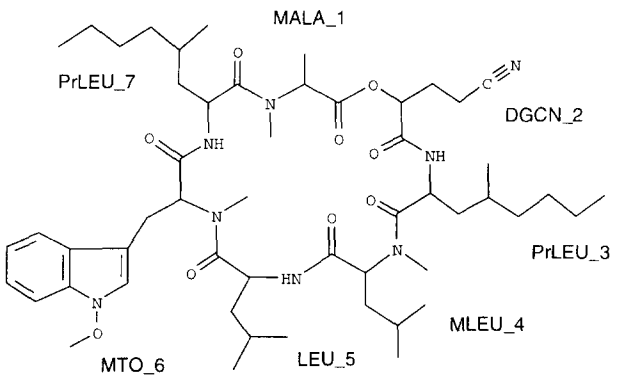

Fig. 1. Schematic representation of HUN-7293.

$g \cdot cm^{-3}$. 10096 reflexions were measured out to a resolution of 0.89 Å ($\theta < 60°$, CuKα radiation), which yielded 5133 unique reflexions ($R_{int} = 0.082$), of which 3151 with $|F_o| > 4\ \sigma(F)$. The intensities were corrected for a slow decay of the crystal during measurement (15.7% in 154 h of exposure time). No absorption correction was applied ($\mu = 8.9\ cm^{-1}$).

3. Results

3.1. Preliminary characterization by NMR

Initial inspection of ROESY spectra showed that HUN-7293 exists in $CDCl_3$/DMSO solutions predominantly in one conformation (>90%). The same observation was made for protic solvent mixtures of MeOH/H_2O, while a higher degree of a second conformation (20%) was found in pure $CDCl_3$ solutions. Prominent structural features of the major conformation are two *cis*-peptide bonds between residues PrLEU_3 and MLEU_4 as well as LEU_5 and MTO_6 (Fig. 2), and large coupling constants $^3J_{HN\alpha}$ and $^3J_{\alpha\beta}$ for some of the residues (Table 1). In addition, there are strong chemical shift shielding effects for the β_1 proton of LEU_5. These results, together with the observation of a slowly exchanging amide proton of PrLEU_7, indicated that the compound exists in a rather fixed conformation under the conditions studied.

3.2. NMR structure determination

For calculation of the solution structure of HUN-7293, a total number of 78 NOE-derived distance restraints were extracted from ROESY spectra; 27 intraresidual, 26 sequential ($|i-j| = 1$), and 25 medium range ($1 < |i-j| < 4$). In addition, 5 angle restraints (2ϕ, $3\ \chi_1$) were derived from measurement of coupling constants and inspection of internuclear distances using GLOMSA [13]. A set of 20 individual structures was then calculated on the basis of these restraints using standard simulated annealing protocols in X-PLOR. Most of the structures (19/20) converged to the same fold with no violations to the experimental distance restraints greater than 0.35 Å and dihedral restraints greater than 5°. The atomic root-mean-square deviation of ten structures with lowest energies (<20 $kcal \cdot mol^{-1}$) was 0.08 Å and 0.44 Å for backbone atoms and heavy atoms, respectively. The structure can thus be described as well defined for both the backbone and some of the sidechain conformations (Fig. 3).

3.3. Solvent dependence of the 3D structure

A pertinent question in our study was whether the three-dimensional structure of HUN-7293, determined in aprotic apolar solution, is also relevant under physiological conditions. To address this issue, we checked its conformational properties qualitatively in a polar and protic solvent mixture (MeOH/H_2O: 70%/30%) since the compound is not soluble in water. Several lines of evidence suggest that a conformation very similar to the one calculated for organic solvent mixtures can be assumed to also exist in aqueous solutions. This assumption is based on the experimental observations of the same two *cis*-peptide bonds (Fig. 2), the similar coupling constants (Table 1), the characteristic chemical shift for the β_1 proton of LEU_5 (−0.61 ppm in $CDCl_3$/DMSO; −0.71 ppm in MeOH/H_2O) induced by ring current shift effects mediated by stacking interactions with the neighboring MTO_6, and the slow exchange of NH of PrLEU_7 with bulk solvent.

3.4. X-Ray structure analysis

Crystallization of HUN-7293 proved to be cumbersome ini-

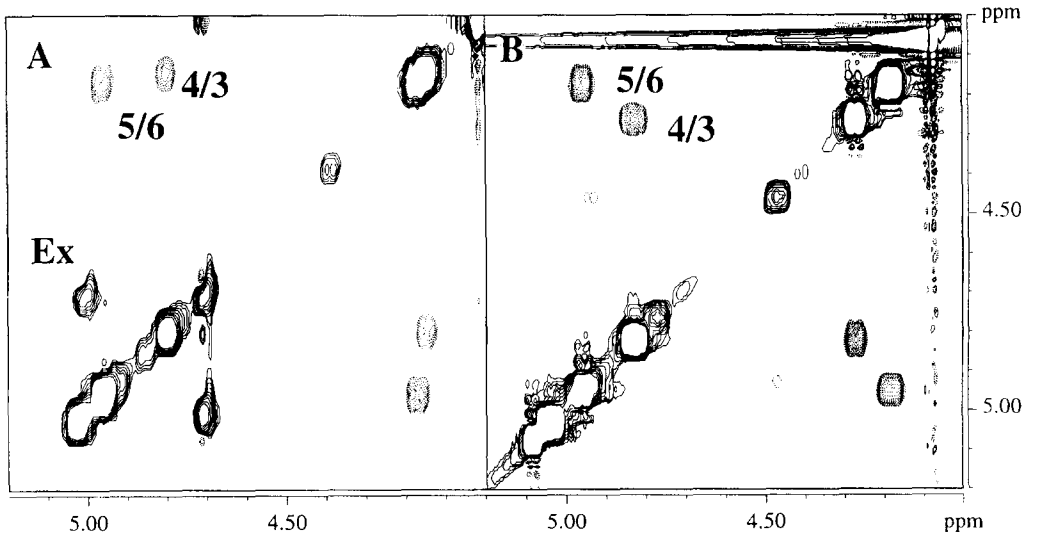

Fig. 2. Part of a ROESY spectrum of HUN-7293 acquired in (A) 70% CD_3OD/30% D_2O and (B) 80% $CDCl_3$/20% (D_6)DMSO. The negative cross-peaks between the CaH resonances of residues 3, 4 and 5, 6 indicating the two *cis*-peptide bonds are labelled according to the residue position; the additional positive cross-peak (Ex) in (A) is due to chemical exchange of the solvent OH resonances.

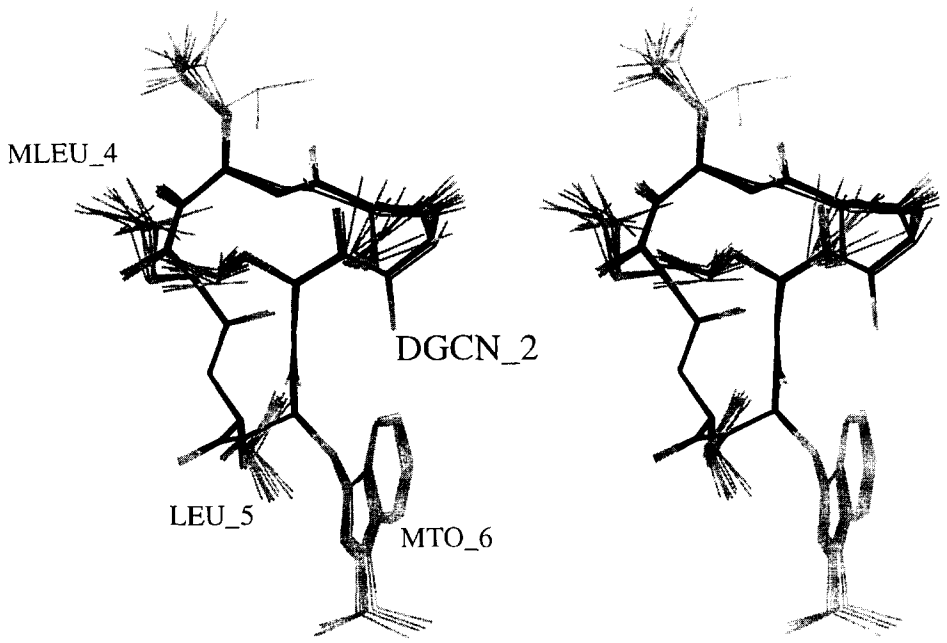

Fig. 3. Stereo-picture of the solution structure of HUN-7293. The backbone atoms (Cα, C, N) of 10 selected structures with lowest total energies (<20 kcal·mol^{-1}) have been best fit superpositioned with a root-mean-square deviation of 0.08 Å. The backbone is shown in heavy lines and side chain atoms are shown in grey (note that the PrLEU residues have been truncated for structure calculation purposes by leucine residues in the NMR study). The final values of each term of the target function were: F_{tot} = 22.0 ± 5.6 kcal·mol^{-1}; F_{bonds} = 2.8 ± 0.6 kcal·mol^{-1}; F_{angle} = 8.1 ± 2.8 kcal·mol^{-1}; $F_{improper}$ = 1.0 ± 0.8 kcal·mol^{-1}; F_{vdW} = 2.8 ± 0.4 kcal·mol^{-1}; F_{noe} = 7.4 ± 1.2 kcal·mol^{-1}; F_{dhi} = 0.02 ± 0.03 kcal·mol^{-1}.

tially, and as a consequence the structure determination was carried out after the high resolution NMR structure in solution was completed. As described above, well-diffracting crystals could be grown from a solvent mixture containing 80% DMSO. This is consistent with the observation made in the solution studies which showed that HUN-7293 can be stabilized in one conformation by an aprotic solvent such as DMSO.

The structure was solved by direct methods using SHELXS-86 [15] and refined by Full Matrix LS-methods (SHELX-76, [16]) to an *R*-factor of 0.0928 for 751 structural parameters (anisotropic temperature factors for all heavy atoms, H-atoms 'riding' on the attached atom) for 3151 structure factors with $|F_o|>4\ \sigma(F)$ (R_w = 0.1046, S = 1.308, average shift/esd in final cycle = 0.15). In the final difference Fourier there was no electron density above 0.33 e·Å^{-3}.

During the refinement a solvent molecule of DMSO was detected in the electron density and subsequently included in the calculations. A positional disorder of the *N*1′-*O*-methylindol moiety of MTO was also found: the fragment existed in two orientations flipped by 180° around χ_2, thus having a common

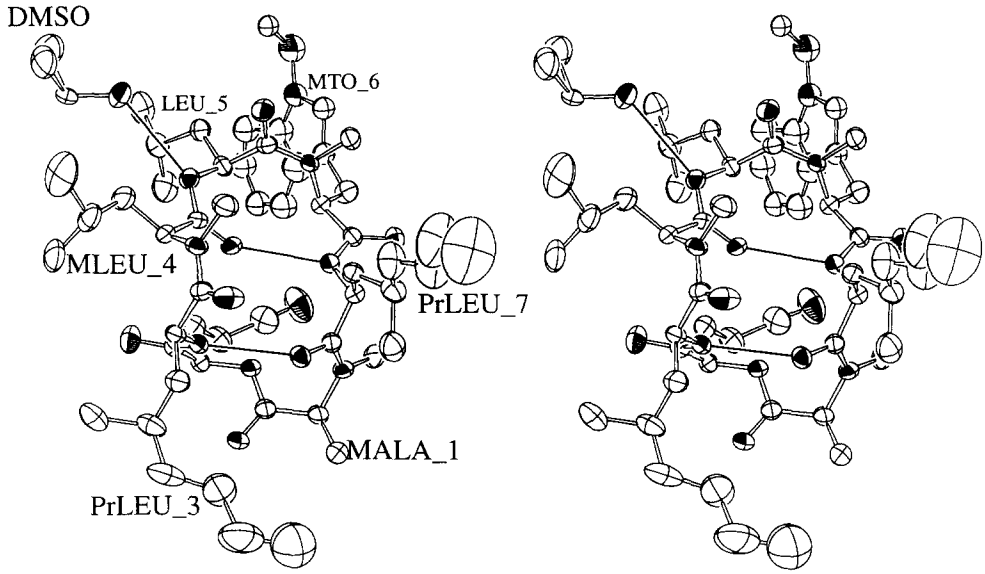

Fig. 4. ORTEP stereo-view of the crystal structure of HUN-7293. Non-hydrogen atoms are shown as 25% probability thermal ellipsoids. The transannular hydrogen-bonds are shown by thin lines.

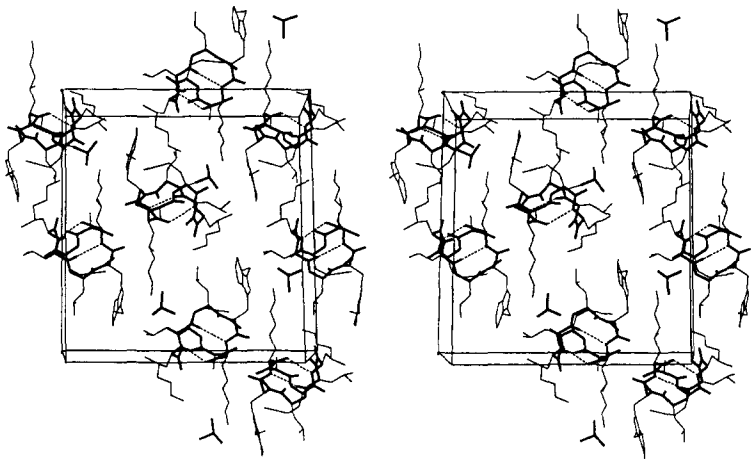

Fig. 5. Stereo-diagram indicating the crystallographic packing of HUN-7293. The backbone is highlighted by heavy lines.

plane for the two positions. (For clarity only one position with $\chi_2 = 81°$ is shown in the Figures.)

3.5. Crystalline conformation

An ORTEP stereo-view of the molecular conformation of HUN-7293 is depicted in Fig. 4, indicating the 25% probability thermal vibration ellipsoids. It clearly shows the well-defined positions of the cyclic backbone and the growing thermal vibration of atoms with increasing distance from the backbone, most prominent for the extended PrLEU sidechains. The backbone conformation is very similar to the solution structure and is characterized by the two *cis*-amides (PrLEU_3 to MLEU_4, and LEU_5 to MTO_6), and the two strong transannular hydrogen bonds adding stability to the backbone (Table 2). Also shown in Fig. 4 is the solvent molecule DMSO, whose oxygen is in hydrogen bonding distance to the NH of LEU_5, d(O...H-N) = 3.07 Å. Analysis of the intermolecular contacts revealed no other short interactions apart from the hydrogen bond mentioned above; in fact, no other hydrogen bonds would be possible since no additional exposed H-bond donors exist. The crystal packing diagram is shown in Fig. 5.

The absolute configuration of HUN-7293 was assumed from the known chirality of its constituent L-LEU_5, identified experimentally (data not shown). The X-ray analysis proved that all α-amino acids in the compound have L-configuration, in particular the novel PrLEU and MTO amino acids. The 2-hydroxy acid DGCN_2, however, has D-configuration. This approach also verified the R-chirality of the Cγ in the side chains of PrLeu.

4. Discussion

The structure of HUN-7293 is best described as an 'erected Cobra-head', depicted in Fig. 3. One can also think of an image where the backbone of the molecule follows the outline of a hand with the fingers closed and the palm forming a hollow. The *cis*-peptide bond between residues 5 and 6 would be located at the wrist, while the fingertips would point towards residues 2 and 3. This overall bent structure allows residues DGCN_2, LEU_5 and MTO_6 to come in close proximity to one another on one face of the peptide. We also note that both 'C9-amino' acids point into the same direction on the opposite face of the molecule. The calculated structures satisfy other experimental observations than those used for the structure calculations. A hydrogen bond observed between the NH of PrLEU_7 and C = O of MLEU_4 in both the solution and the crystal structure explains the slow exchange of this proton with bulk solvent. A second hydrogen bond between NH of PrLEU_3 and C = O of PrLEU_7 is present in the crystal but not the solution structure, and consequently the proton involved was found to rapidly exchange with bulk solvent in solution. Furthermore, strong ring current shift effects for the β_1 proton of LEU_5 indicate stacking interactions with the indole moiety of MTO_6, as seen in both the crystal and solution structure.

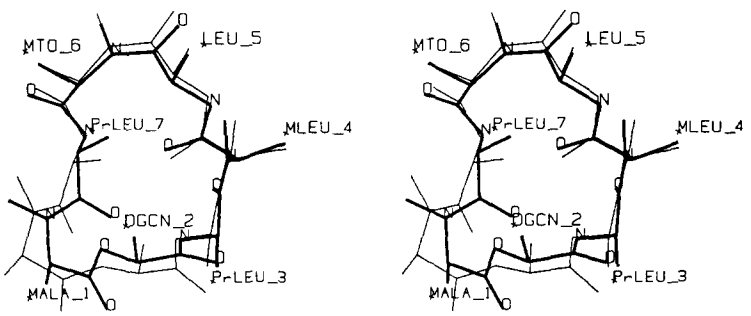

Fig. 6. Best fit superposition of the backbone of the crystal structure (heavy lines) on the energy minimized average solution structure (thin lines) of HUN-7293.

Table 1
Comparison of coupling constants in different solvents: A (80% $CDCl_3$/20% (D_6)DMSO), B (70% CD_3OH/30% H_2O) $\beta1$ and $\beta2$ refer to the low-field or high-field component of a β-methylene group, respectively

Residue	Solvent A			Solvent B*		
	$^3J_{HN\alpha}$ (Hz)	$^3J_{\alpha\beta1}$ (Hz)	$^3J_{\alpha\beta2}$ (Hz)	$^3J_{HN\alpha}$ (Hz)	$^3J_{\alpha\beta1}$ (Hz)	$^3J_{\alpha\beta2}$ (Hz)
2			3.0		9.5	3.5
3	9.8	8.0	6.0	9.4	8.0	6.0
4		11.5	3.5		11.5	4.0
5	6.4	12.0	3.5	6.0		3.5
7	9.8	9.5	5.0	10.3	9.0	5.0

*Fully deuterated solvents have been used for measurement of $^3J_{\alpha\beta1}$ and $^3J_{\alpha\beta2}$.

Table 2
Hydrogen bonds observed in the crystal structure of HUN-7293

D-H...A	d(D...A) (Å)	d(H...A) (Å)	a(D_H...A) (degree)
N(7)-H...O = C(4)	2.80	1.75	165
N(3)-H...O = C(7)	2.82	1.77	164

Inspection of the structure also provides insight into possible functional regions of the molecule. In general, there are only a few polar groups found on the surface of the molecule which are accessible for a putative hydrogen bond acceptor/donor of the HUN-7293 receptor. One possible hydrogen-bond donor is the NH group of residue LEU_5, and interestingly, a solvent molecule was found to be in hydrogen-bonding distance in the crystal structure. Other polar groups found on the surface of the molecule are the carbonyl groups of MALA_1, DGCN_2, LEU_5 and MTO_6 which represent possible hydrogen bond acceptors. In addition, the 4-cyano group of DGCN_2 is solvent exposed and thus appears to be a possible anchor for ligand receptor interactions.

Availability of both a solution and crystal structure of HUN-7293 opens the way for studying potential receptor-induced conformational changes of the compound. As shown in Fig. 6, both the crystal and solution structure of HUN-7293 are very similar. The root-mean-square deviation between the crystal and energy minimized average solution structure is 0.37 Å (C, N, Cα, Cβ, CN, O) of residues 1–7, and 0.28 Å for residues 3–7. The larger deviations seen around residue DGCN_2 are accompanied by the formation of a hydrogen bond between NH of PrLEU_3 and C = O of PrLEU_7 in the crystal structure, which is not present in the solution structure. In addition, the side-chain of residue 2, which is in close proximity to the side chain of residue 6, radiates slightly off from the macrocycle in the crystal structure. It is therefore tempting to speculate that the observed changes reflect the situation when HUN-7293 binds to its cognate receptor. Further structural studies on HUN-7293 derivatives are needed, however, to exclude the possibility that the minor changes seen are induced by crystallographic packing rather than a genuine induced-fit binding mode.

Acknowledgements: We would like to thank Drs. E. Küsters for determining the absolute stereochemistry of some HUN-7293 residues, G. Seidel for the initial crystallization, A. Widmer for help with in-house development of software tools, and C. Dalvit for providing NMR pulse programmes.

References

[1] Springer, T.A. (1994) Cell 76, 301–314.
[2] Carlos, T.M. and Harlan, J.M. (1994) Blood 84, 2068–2101.
[3] Winiski, A.P. and Foster, C.A. (1992) J. Invest. Dermatol. 99, 48–52.
[4] Foster, C.A, Dreyfuss, M., Mandak, B., Meingassner, J.G., Naegeli, H.U., Nussbaumer, A., Oberer, L., Scheel, G. and Swoboda, E.-M. (1994) J. Dermatol. 21, 847–854.
[5] During the preparation of this manuscript, Patent JP07109299 –a claiming anti-HIV activity for the same fungal metabolite was published.
[6] Borel, J.F., Di Padova, F., Mason, J., Quesniaux, V., Ryffel, B. and Wenger, R. (1989) Pharm. Rev. 41, 239–242.
[7] Schreiber, S.L. and Crabtree, G.R. (1992) Immunol. Today 13, 136–142.
[8] Kingston, D.G.I. (1994) Trends Biotechnol. 12, 222–227.
[9] Wu, T.W., Ali, F.E.,Barton, L.S., Bean, J.W., Bondinell, W.E., Burgess, J.L., Callahan, J.F., Calvo, R.R., Chen, L., Eggleston, D.S., Gleason, J.G., Huffman, W.F., Hwang, S.M., Jakas, D.R., Karash, C.B., Keenan, R.M., Kopple, K.D., Miller, W.H., Newlander, K.A., Nichols, A., Parker, M.F., Peishoff, C.E., Samanen, J.M., Uzinskas, I. and Venslavsky, J.W. (1993) J. Am. Chem. Soc. 115, 8861–8862.
[10] Gurrath, M., Müller, G., Kessler, H., Aumailley, M. and Timpl, R. (1992) Eur. J. Biochem. 210, 911–921.
[11] Bothner-By, A.A., Stephens, R.L., Lee, J.M., Warren, C.D. and Jeanloz, J.W. (1984) J. Am. Chem. Soc. 106, 811.
[12] Bartels, C., Xia, TH., Billeter, M., Güntert, P. and Wüthrich, K. (1995) J. Biomol. NMR 6, 1–10.
[13] Güntert, P., Braun, W. and Wüthrich, K. (1991) J. Mol. Biol. 217, 517–530.
[14] Brünger, A.T. (1992) in: Xplor Manual V3.0, Yale University, New Haven, CT.
[15] Sheldrick, G.M. (1985) SHELX86. Program for Solution of Crystal Structures, Univ. of Göttingen, Germany.
[16] Sheldrick, G.M. (1976) SHELX76. Program for Crystal Structure Determination, Univ. of Cambridge, UK.